"Physics of Auroral Phenomena", Proc. XLV Annual Seminar, Apatity, pp. 16-19, 2022

Polar Geophysical Institute

DOI: 10.51981/2588-0039.2022.45.003

MAGNETIC STORM ON 20 APRIL 2020: SPATIAL DEVELOPMENT OF THE SUBSTORM IN THE MAIN PHASE

L.I. Gromova[1], N.G. Kleimenova[2], I.V. Despirak[3], S.V. Gromov[1], A.A. Lubchich[3], L.M Malysheva[2]

[1]*Pushkov Institute of Terrestrial Magnetism, Ionosphere, and Radio Wave Propagation, Moscow, Troitsk, Russia;* e-mail*: gromova@izmiran.ru*
[2]*Schmidt Institute Physics of the Earth RAS, Moscow, Russia*
[3]*Polar Geophysical Institute, Apatity, Russia*

Abstract. The global features of the spatial-temporal distribution of high-latitude geomagnetic disturbances during the main phase of the first magnetic storm (20 April 2020) of the new, 25-th cycle of the solar activity have been studied. Basing on the ground based measurements by the global networks SuperMAG, INTERMAGNET and satellite data of AMPERE project (Active Magnetosphere and Planetary Electrodynamics Response Experiment), it was shown that the geomagnetic disturbances during this storm was significant (Kp = 5) despite the low speed of the magnetic cloud caused this storm. The intense (the peak intensity > -1000 nT) auroral substorm was observed in the storm main phase. The scenario of this substorm likes to the scenario of the supersubstorm (the peak intensity ~-2500 nT) in the main phase of the magnetic storm on 28 May 2011 when the conditions of the interplanetary magnetic field (IMF) were similar but the speed and dynamic pressure of the solar wind were slight higher. It was supposed that spatial development of the intense substorms during a storm main phase depends more on the appearance of large values of the southward IMF than on the speed and dynamic pressure of the solar wind and the global large-scale distribution is the common behavior of the intense substorm (*SML*-peak intensity~ -1000 nT) as well as of the supersubstorm (*SML*-peak intensity ~-2500 nT).

Introduction

The first magnetic storm in the beginning of the new 25-th solar activity cycle occurred on 20 April 2020. It was associated with a *slow* magnetic cloud (*MC*) approached the magnetosphere of the Earth. The detailed overview of the solar event caused this magnetic cloud and, as a result, the considered magnetic storm, was reported in [*Davies et al.*, 2021; *O'Kane et al.*, 2021]. Usually, geoeffectiveness of *slow* magnetic clouds (V < 400 km/s according to [*Tsurutani et al.*, 2004]) is low, they do not cause intense storms [*Richardson and Cane*, 2012]. But in this case, *MC* was also characterized by significant amplitude of the southward IMF (the IMF *Bz* reached -15 nT). Apparently, this led to the development of a moderate magnetic storm with the peak *SYM/H* ~ -70 nT.

There are lot of works studying intense magnetic storms caused by *fast* magnetic clouds, e.g., [*Tsurutani et al.*, 1992; *Kleimenova et al.*, 2021, and references therein]. But magnetic storms associated with *slow* magnetic clouds have not been studied enough, as well as their high-latitude geomagnetic effects. e.g., [*Nitta et al.*, 2021]. In [*Gromova et al.*, 2022], it was shown that geoeffectiveness of the storm 20 April 2020 was rather high. It was discussed the geomagnetic disturbances in the morning-daytime sector of the polar latitudes (>70° MLAT) and some features of substorms during the initial and main phases of the magnetic storm.

The aim of this paper is to study the global features of the spatio-temporal distribution of the intense substorm in the main phase of the storm on 20 April 2020 in the comparison with the scenario of the supersubstorm in the main phase of the magnetic storm on 28 May 2011 whose main phase occurred at approximately the same UT.

Observations and discussion

The variations of the IMF components *By*, *Bz* and the speed (*V*) and dynamic pressure (*Psw*) of the solar wind on 20 April 2020 and 28 May 2011 are shown in Figure1a. The main phase of the storm on 20 April 2020 was developed after the sharp southward turn of the IMF *Bz* (to -15 nT) that does not changed for about 4 hours under the unstable IMF *By*. At the same time the dynamic pressure of the solar wind dropped to 2 nPa, the solar wind speed remained low, ~350-380 km/s. The IMF conditions in the main phase of the storm on 28 May 2011 were similar but the speed and dynamic pressure of the solar wind were slight higher (~500 km/s and~4 nPa respectively).

The variation of the *SML*-index in Figure1b display the intense substorm in the main phase of the storm on 20 April 2020 and the supersubstorm (*SSS*) during the main phase of the storm on 28 May 2011. As-the peak intensity of the substorm as the supersubstorm one were observed under the significant negative IMF *Bz* and *By* and when some other parameters of the solar wind (*V* and *Psw)* were close. It made possible to compare development of the observed substorm and supersubstorm. The development of the supersubstorm in the main phase of the storm on 28 May 2011 was studied in [*Despirak et al.*, 2022].

In Figure 2a, the spatio-temporal distribution of the intense substorm with comparison with the same of supersubstorm is demonstrated with AMPERE-maps constructed with registrations by the Iridium constellation of 66 satellites at 780 km altitude, distributed over six orbit planes spaced equally in longitude. The AMPERE-maps of the ionospheric currents (auroral electrojets) show that they developed in a similar way during the substorm(left) and supersubstorm (right) peak intensity. The intense and extended westward electrojet is observed in the midnight, morning, and dayside sectors and the intense eastward electrojet was observed in the afternoon and evening sectors, as it is typically for supersubstorms. But the maps of the Field-Aliened Currents (FACs) distribution show their enhancement as well. Notes, in the both events, the daytime-morning FACs demonstrate the complex latitude layered structure that could be caused geomagnetic disturbances in the polar latitudes in the morning and dayside sectors.

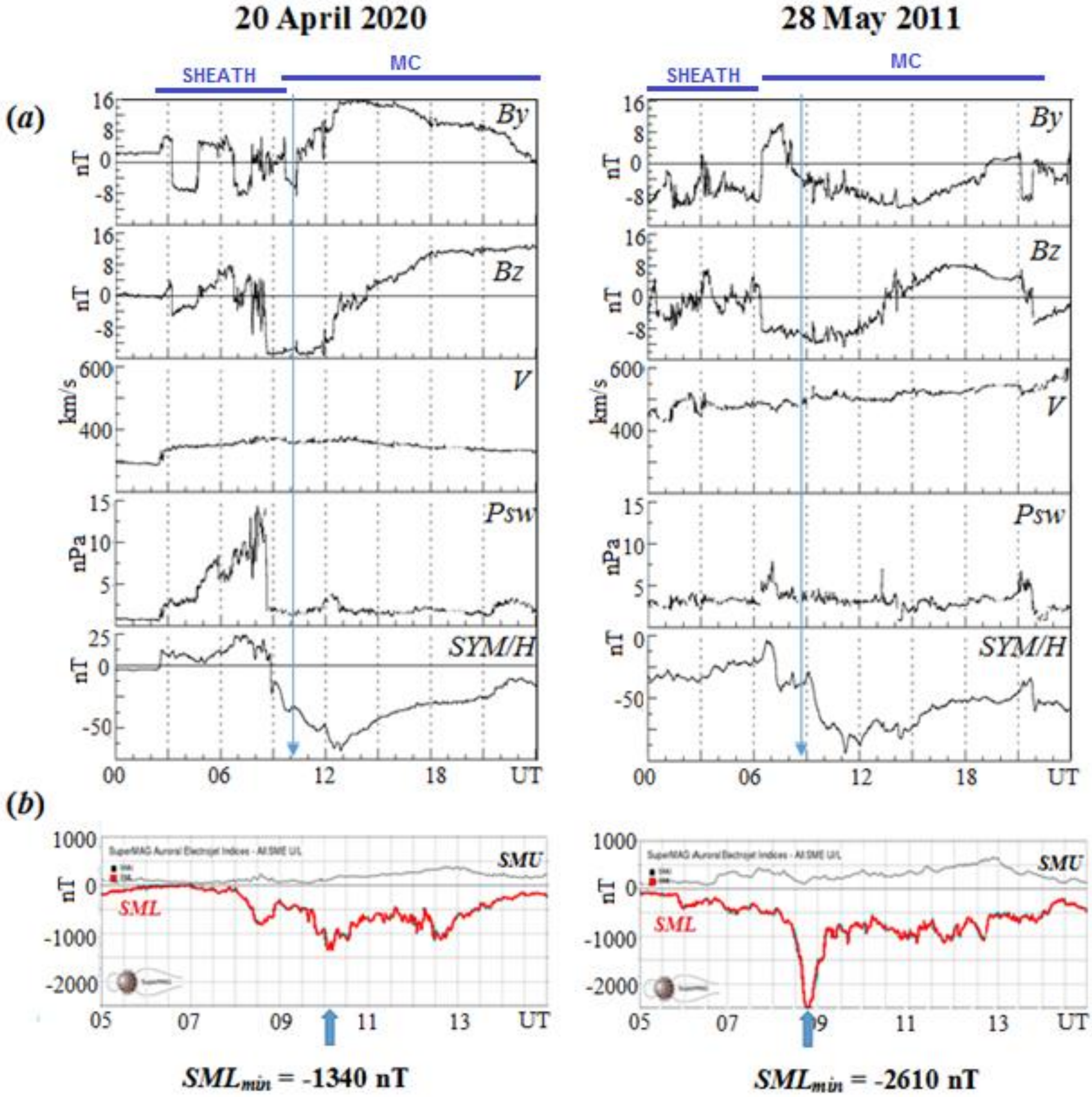

Figure 1. (*a*) Variation of the IMF *By*, *Bz*, the solar wind speed (*V*) and dynamic pressure (*Psw*), the global index of the geomagnetic activity *SYM/H* (1-min analog of *Dst*-index) on 20 April 2020 (left) and 28 May 2011(right). The boundaries of *SHEATH* regions and the *MCs* according to the catalog of the large-scale solar wind phenomena are indicated by blue bars. Thin blue arrow points the peak intensity of the substorm and supersubstorm; (*b*) variation of *SML*-index in 05-14 UT of 20 April 2020 (left) and 28 May 2011 (right). Thick blue arrow points the peak intensity of the substorm and the supersubstorm. Here we used the *SML*-index constructed from SuperMAG data (included more than 100 stations in between 40° and 80° MLAT) as a proxy of a substorm intensity instead of *AL*-index. Data from https://omniweb.gsfc.nasa.gov/, http://iki.rssi.ru/pub/omni/catalog/, https://supermag.jhuapl.edu/.

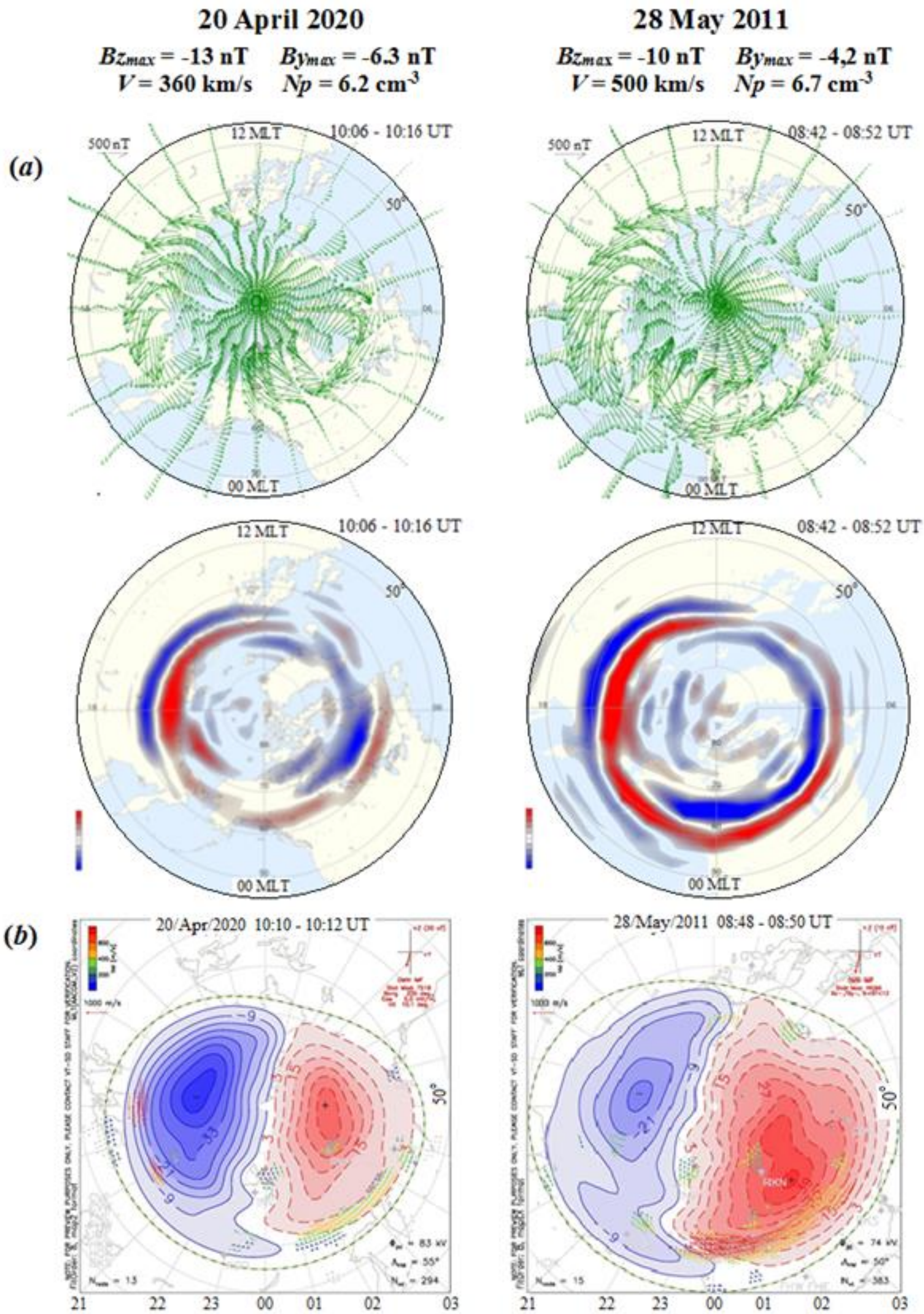

Figure 2. The peak intensity of the substorm (left) and supersubstorm (right). (*a*) AMPERE–derived maps of the spherical harmonic analysis of magnetic measurements, vectors of the magnetic field were rotated 90° clockwise to indicate ionospheric equivalent current direction, and *FAC* densities during the peak intensity of the substorm and supersubstorm; red and blue color shows the upward and downward currents respectively; (*b*) SuperDARN ionospheric convection maps along with *DP*2 contours at the same interval. Data from http://www.ampere/jhapl.edu; http://vt.superdarn.org/.

The ionospheric currents presented as SuperDARN convection maps (see Figure2b) in the peak intensity of the substorm and supersubstorm could be considered as twin-vortices current system *DP*2 with two large-scale convection vortices. As it is reported in [*Kumar et al.*, 2020] under southward *Bz* and when the IMF *By* is negative, the dusk cell (negative) is stronger than dawn cell (positive). In our case, it is seen that the dusk cell of convection was stronger on 20 April 2020 than on 28 May 2011.

Summary

The first magnetic storm in the new solar activity cycle was caused by *slow* magnetic cloud, but large negative values of the IMF *Bz* led to the significant geomagnetic activity expressed in the development of geomagnetic disturbances in the morning-dayside sector of the polar latitudes in the initial phase of the storm and intense substorm in the main phase that comparable with the supersubstorm on 28 May 2011.

It is shown that the intense substorm (SML_{min} = -1340 nT) observed in the main phase of the magnetic storm on 20 April 2020 developed globally. Its spatial-temporal distribution was similar the scenario of the supersubstorm on 28 May 2011.

We found that the global scale distribution is common behavior of the intense substorm (*SML*-peak intensity > -1000 nT) as well as of the supersubstorm (*SML*-peak intensity ~-2500 nT).

References

Davies E.E., Möstl C., Owens M.J., et al. (2021). In situ multi-spacecraft and remote imaging observations of the first CME detected by Solar Orbiter and BepiColombo, A&A, Vol 656, id. A2. https://doi.org/10.1051/0004-6361/202040113

Despirak I.V., Kleimenova N.G., Lyubchich A.A., et al. (2022). Global development of the supersubstorm of May 28, 2011, Geomagn. Aeron., Vol 62, No 3, pp. 325-335. https://doi.org/10.1134/S0016793222030069

Gjerloev J.W. (2012). The SuperMAG data processing technique, J. Geophys. Res., Vol 117, A09213. https://doi.org/10.1029/2012JA017683

Gromova L.I., Kleimenova N.G., Levitin A.E., et al. (2016). Daytime geomagnetic disturbances at high latitudes during a strong magnetic storm of June 21–23, 2015: The storm initial phase, Geomagn. Aeron., Vol 56, No 3, pp. 302-313. https://doi.org/10.1134/S0016793216030051

Gromova L.I., Kleimenova N.G., Despirak I.V., et al. (2022). Polar geomagnetic disturbances and auroral substorms during the magnetic storm on 20 April 2020, Proceedings of the Fourteenth Workshop "Solar Influences on the Magnetosphere, Ionosphere and Atmosphere" June, pp. 16 – 21. https://doi.org/ 10.31401/WS.2022.proc

Hajra R., Tsurutani B.T., Echer E., Gonzalez W.D., and Gjerloev J.W. (2016). Supersubstorms (SML < _2500 nT): Magnetic storm and solar cycle dependences, J. Geophys. Res.: Space Physics, Vol 121, pp 7805–7816. https://doi.org/10.1002/2015JA021835

Kleimenova N.G., Gromova L.I., Gromov S.V., et al. (2021). High-Latitude geomagnetic disturbances and field-aligned currents in the recovery phase of the large magnetic storm, Geomagn. Aeron., Vol 61, No 4, pp 520-528. https://doi.org/10.31857/S0016794021040076

Nitta N.V., Mulligan T., Kilpua E.K. (2021). Understanding the origins of problem geomagnetic storms associated with "Stealth" coronal mass ejections, Space Sci. Rev., Vol 217, id. 82. https://doi.org/10.1007/s11214-021-00857-0

O'Kane J., Green L. Davies E., et al. (2021). Solar origins of a strong stealth CME detected by Solar Orbiter, A&A, Vol 656, id. L6. https://doi.org/10.1051/0004-6361/202140622

Kumar S., Veenadhari B., Chakrabarty D., et al. (2020). Effects of IMF By on ring current asymmetry under southward IMF *Bz* conditions observed at ground magnetic stations: Case studies, J. Geophys. Res.: Space Physics, Vol 125, e2019JA027493. https://doi.org/0.1029/2019JA027493

Richardson I.G., Cane H.V. (2012). Solar wind drivers of geomagnetic storms during more than four solar cycle, J. Space Weather Space Clim., Vol 2, A01. https://doi.org/10.1051/swsc/2012001

Tsurutani B.T., Gonsalez W.D., Tang F., et al. (1992). Great magnetic storms, Geophys. Res. Lett., Vol 9, pp.73-76. https://doi.org/10.1029/91GL02783

Tsurutani B.T., Gonzalez W.D., Zhou X.-Y., et al. (2004). Properties of slow magnetic clouds, JASTP, Vol 66, No 2, pp 147-151. https://doi.org/10.1016/j.jastp.2003.09.007